

MonkeyTree: Near-Minimal Congestion for Multi-tenant Training via Migration

Anton A. Zabreyko

Weiyang Wang

Manya Ghobadi

MIT

ABSTRACT

We present MonkeyTree, the first system to mitigate network congestion in multi-tenant GPU clusters through job-migration based *defragmentation* rather than network-layer techniques. As cloud operators co-locate ML training jobs on shared, over-subscribed networks, congestion degrades training throughput for over a third of jobs. Prior approaches either rely on routing and flow scheduling—which we show have fundamental limits when traffic exceeds capacity, or require costly full-bisection bandwidth topologies with packet spraying.

MonkeyTree exploits characteristics of ML training traffic: ring-based collectives generate exactly one cross-rack flow per rack a job spans, making congestion-free placements *achievable*. The sparse constraint structure admits abundant valid configurations, making them *easy to reach* with few migrations. Once reached, low fragmentation is *self-reinforcing*, as new arrivals disturb only a few racks. MonkeyTree formulates defragmentation as an integer linear program that minimizes worker movements, subject to per-rack fragmentation bounds. We prove a tight bound showing any placement can be defragmented to at most two cross-rack fragments per ToR, and extend the formulation to hybrid parallelism with multiple rings per server. Migration is implemented via in-memory checkpoint-and-restore over RDMA, incurring only 9.02 seconds of system overhead end-to-end per worker. We evaluate MonkeyTree using a custom simulator modeling clusters of up to 2,048 H200 GPUs and prototype on a five-node A100 testbed. MonkeyTree improves average job completion time by 14% over the next best baseline on a cluster of 1,024 GPUs with a 4:1 oversubscription. With a high 16:1 oversubscription ratio and 2,048 GPUs, MonkeyTree keeps p99 job completion time within 5% of ideal.

1 INTRODUCTION

Multi-tenant GPU clusters have become a common deployment model for machine learning (ML) training workloads in the cloud [9, 53, 55, 59, 67, 72]. In such environments, network congestion is a persistent challenge: concurrent jobs compete for shared bandwidth, degrading training throughput of 36.1% of the jobs [9]. The problem is compounded by the fact that operators traditionally build oversubscribed datacenter networks to reduce cost, further limiting available capacity during traffic bursts [19, 54, 60].

Prior work has tackled this problem from two directions. The first is to leverage routing [9, 53, 59, 73] and flow-scheduling [55, 57] techniques to mitigate congestion by selecting efficient paths and time-multiplexing network resources across jobs. However, we demonstrate that these approaches have fundamental limits: when aggregate traffic exceeds network capacity, flow collisions become inevitable even with optimal routing and flow scheduling (§2). At the other extreme, industry leaders are pushing packet spraying over full-bisection bandwidth topologies as the ultimate solution [7, 14, 15, 63]. This network architecture provides near-ideal performance, but at substantial cost. Achieving full-bisection bandwidth requires a large number of network switches, and packet spraying demands specialized switches and NICs [47]. Cloud providers must therefore trade performance against infrastructure expense.

We analyze the traffic patterns of multi-tenant DNN training jobs and show that traffic is dominated by *sparse* elephant flows, in which each GPU communicates with only one other GPU for the majority of its traffic. This sparsity suggests network congestion is *rare*, even on oversubscribed networks. In practice, however, jobs are often *fragmented* across servers in different racks. Such fragmentation persists under high load despite locality-aware job schedulers (§2), causing the flow count on ToR-to-spine links to spike and increasing network load by 4.85× relative to optimal placement (§6.3). This leads to congestion despite sparse per-job traffic. Existing mitigation approaches address this only through networking techniques [9, 53, 55, 57, 59, 73], but do not tackle the root cause, leaving clusters persistently fragmented.

We argue that the most effective way to address congestion in multitenant GPU clusters lies not in optimizing network transfers but in *job placement*. Based on this insight, we propose MonkeyTree, a system that continuously maintains a low-fragmentation state through small, proactive job *migrations*—moving workers of the same job to concentrate them on the same racks. This *defragmentation* reduces competing network traffic at its root cause, rather than reacting to congestion after it arises.

Using job migration to reduce congestion in GPU clusters remains unexplored, a legacy of CPU-centric datacenters. However, CPU workloads generate arbitrary traffic matrices, making congestion-free placements both ill-defined and rare. Reaching a defragmented placement that minimizes network

traffic requires migrating a large fraction of workers, yet contention persists because no placement isolates traffic from workers entirely (§2.2). We argue that GPU training traffic is fundamentally different, and migration-based defragmentation is not only practical but highly effective for multi-tenant ML clusters, requiring only a small number of targeted migrations to eliminate congestion. MonkeyTree rests on three key insights about the structure of ML training traffic:

First, congestion-free states are *achievable* in GPU clusters. The majority of ML training traffic consists of ring-based collectives that generate exactly one flow per rack a job spans. This property transforms the problem: rather than minimizing network traffic, we need only keep each rack’s outgoing flows below its uplink count. Any placement satisfying this constraint achieves full path isolation.

Secondly, congestion-free states are *abundant*. Unlike CPU workloads, where low-traffic placements are rare, the sparse constraint structure for GPU training admits many valid congestion-free configurations. Worker ordering and placement within racks do not affect traffic patterns, and each rack’s constraint is independent. These degrees of freedom make congestion-free states easy to reach from any starting point.

Finally, maintaining low fragmentation is *self-reinforcing*. Once a cluster reaches a valid state, maintaining it requires minimal effort. A new job can violate constraints at only a few racks, and because valid placements are abundant, a small number of migrations restores compliance.

Building on these insights, MonkeyTree employs a centralized controller and distributed daemons that operate alongside existing job schedulers without modifying their placement logic (§4). When jobs arrive, the scheduler assigns GPUs as usual. MonkeyTree monitors the resulting placement and checks whether any rack’s fragmentation exceeds a threshold derived from its uplink count. If so, the controller invokes a migration solver to compute the minimum migrations needed to restore a congestion-free state. Once fragmentation is bound, the controller computes routes using a *Perfect routing* scheme we designed (§5.4), that assigns each DP flow a dedicated uplink, achieving full path isolation. Daemons on each server execute migrations and configure local routing rules. By exploiting ML traffic sparsity and the self-reinforcing nature of low fragmentation, MonkeyTree keeps migration overhead minimal, typically requiring less than two moves per job arrival.

The core algorithmic contribution is the migration solver. We formulate the problem as an integer linear program (ILP): given a current placement, find a new placement that meets the fragmentation target while minimizing worker movements (§5.2). We first solve this for workloads with a single ring-based collective and prove a tight bound: any placement can be defragmented into at most 2 cross-rack fragments per ToR (§5.1). This bound is both achievable and necessary in the

worst case. Using insights from the proof, we extend the formulation to hybrid parallelism, where each server runs multiple workers forming parallel communication rings (§5.3).

Realizing this design requires addressing two challenges. The first is ILP scalability: integer programs have worst-case exponential complexity. However, our analysis shows that the ILP solve time scales with the number of moves required (§5.2). Combined with the abundance and self-reinforcing nature of low-fragmentation cluster states, the number of moves required is two or less 80% of the time. This keeps solve times low in practice. For a cluster with 1,024 GPUs, solving the ILP takes 0.89 seconds on average, triggered on average every 102 minutes at 80% load (§6.5).

The second challenge is migration overhead. Live migration is considered complex and disruptive, but modern DNN training makes it surprisingly simple. Training frameworks already provide checkpointing to store and restore state for fault tolerance, and we build migration directly on this infrastructure. We implement in-memory checkpoint-and-restore over RDMA using PyTorch’s Distributed Checkpointing library [52].

To evaluate MonkeyTree, we build a custom Rust-based simulator for modeling multi-tenant distributed ML training, modeling clusters of up to 2,048 H200 GPUs and a 400 Gbps network. We implement several models, including variants of GPT-3 [8, 43], GPT-OSS [51], Llama2 [62], and Llama3 [18] (§6.1). We also prototype MonkeyTree in a testbed with five nodes, each equipped with one A100 GPU and a 100 Gbps RDMA NIC, and perform an end-to-end migration benchmark. In simulation, we demonstrate that on a cluster of 1,024 nodes MonkeyTree improves average job completion time by 14% over the next best baseline (§6.2). On a cluster of 2,048 GPUs with an oversubscription ratio of 16:1, we keep the p99 job-completion slowdown to just 5% (§6.4). Our testbed prototypes support efficient migration, with 9.02 s of system overhead from the start of migration to resuming training (§7). To the best of our knowledge, this is the first system to mitigate congestion between competing ML training jobs using migration as the primary remedy. We plan on open-sourcing our codebase upon publication.

This work does not raise any ethical issues.

2 MOTIVATION

2.1 Multi-Tenant Training and Congestion

Multi-tenant training is ubiquitous in today’s cloud environment [9, 53, 55, 57, 59, 73]. A typical GPU cluster consists of GPU servers interconnected by a hierarchical network, shown in Figure 1. Each GPU server contains multiple GPUs, each with a dedicated NIC, as well as an internal high-bandwidth interconnect shown at the bottom of Figure 1. In these shared GPU clusters, each training job occupies one or more GPU

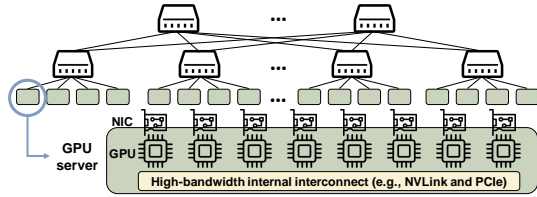


Figure 1: A multitenant GPU cluster.

servers, making the network the primary shared resource. Unfortunately, network congestion significantly degrades training performance, with Alibaba reporting up to 36.1% of the jobs experience throughput reduction due to congestion [9].

Two directions have emerged to address this. The first invests in network infrastructure: packet spraying over full-bisection bandwidth topologies delivers near-ideal performance but requires expensive specialized hardware such as Nvidia's SuperNICs [46, 47]. Many deployments, therefore, accept oversubscribed networks to reduce cost [19, 54, 60]. The second direction employs software techniques, such as routing [9, 53] and flow scheduling [55, 57], to mitigate congestion in oversubscribed networks. We evaluate Crux as an example of these approaches, on a cluster with 1,024 GPUs and 4:1 network oversubscription ratio. We observe a 26% average slowdown despite the mitigation: when aggregate traffic exceeds network capacity, flow collisions become inevitable regardless of strategy. Flow scheduling approaches like Cassini attempt to overlap one job's communication with another's computation, but this strategy is fragile because it requires well-matched job characteristics and becomes unstable when iteration times differ by even a slight amount [58].

Both approaches overlook a more fundamental solution: reducing traffic entering the network in the first place. A job whose workers reside entirely within a single rack generates no traffic beyond the ToR layer, whereas a *fragmented* job spanning multiple racks requires communication through the spine. When too many fragmented jobs share a rack, the aggregate uplink demand exceeds the ToR's uplink capacity, leading to congestion. Job scheduling doesn't resolve fragmentation: our evaluation shows that in a cluster of 1,024 GPUs across 16 racks, up to 93% of ToRs carry more uplink demand than their capacity even under a locality-optimized scheduler. This happens in production systems at scale as well. We analyzed Alibaba's report and found that almost 50% of their jobs are fragmented [9]. The natural remedy is *defragmentation* through job *migration*, yet prior work on network contention in GPU clusters ignores it, a legacy of CPU-centric multitenant clusters where migration was impractical.

2.2 Migration Challenges in CPU Workloads

Migration-based approaches for CPU workloads fall into two categories. The first addresses resource sharing at the server level, where CPU cores and memory are the primary contended resources [16, 24, 69]. Early GPU migration works, such as Gandiva [71], adopted the same granularity, splitting GPUs across jobs on a server. This does not apply to our setting, where the network above between ToR and spine switches is the primary contended resource [9, 20].

The second jointly optimizes placement and routing to reduce network contention [32]. However, CPU workloads generate arbitrary traffic patterns, yielding a multi-objective problem: minimize network traffic while minimizing migrations. This formulation has fundamental limitations. Consider five jobs (color-coded) on 32 servers across eight racks in Figure 2. Each ToR has two uplinks supporting two units of demand, and each node sends one unit of traffic uniformly to others in its job. The initial placement is fragmented, with racks demanding up to 3.8 units (Figure 2, top-left). The placement that minimizes peak per-Tor traffic requires at least 11 migrations (Figure 2, top), yet congestion persists: only two racks stay within uplink capacity, and racks 4 and 7 still exhibit inter-job contention between the green and pink jobs.

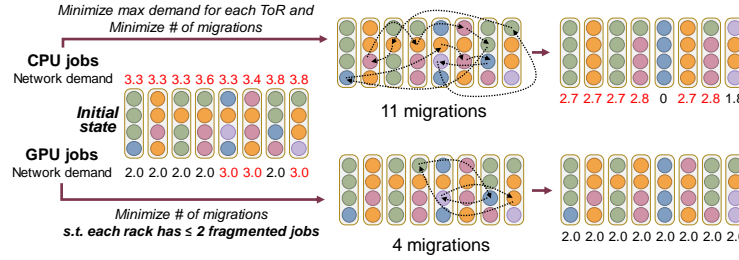
This illustrates two problems. First, eliminating congestion is impossible: no placement achieves zero inter-job contention in this example, and alternative solutions simply shift congestion to different jobs. Without a policy specifying job priorities, there is no clear optimum. Second, good states are sparse: diverse CPU traffic patterns make low-congestion placements rare targets, requiring one-third of the cluster to migrate in this example alone—a ratio that worsens with scale.

In summary, migration for CPU workloads faces fundamental obstacles. Does this change for GPU workloads?

3 TRACTABILITY OF GPU MIGRATION

Distributed training jobs consist of computation and communication operations. Communication arises from parallelizing model training across GPUs, creating data dependencies that manifest as network transfers. Modern LLM training combines multiple parallelization strategies, each generating distinct traffic patterns.

Table 1 shows traffic generated by one iteration of Llama3-70B and GPT3-175B on 128 GPUs with a local batch size of 16. Tensor parallel (TP) traffic is the largest but remains confined to high-bandwidth interconnects such as NVLink within a server. Among traffic entering the datacenter network, data-parallel (DP) collectives dominate: 7.5 \times and 29.4 \times larger than pipeline-parallel (PP) traffic for Llama and GPT, respectively. Congestion, therefore, manifests most significantly when DP collectives from different jobs collide. Hence, we define a placement to be a *congestion-free state* if no DP traffic

**Figure 2: Migration and network congestion in shared CPU vs. GPU clusters.**

Different colors represent workers in different jobs; each ToR switch supports two units of demand. The CPU cluster (top) requires 11 migrations, yet inter-job congestion persists on racks 4 and 7. The GPU cluster (bottom) needs only 4 migrations to eliminate congestion.

Model	Llama3-70B				GPT3-175B					
	Parallelism	Deg.	Total	% of DP	Net?	Parallelism	Deg.	Total	% of DP	Net?
TP		8	35.8 TB	426%	N		8	68.8 TB	3276%	N
DP/FSDP		4	840 GB	100%	Y		4	2.1 TB	100%	Y
PP		4	48 GB	5.7%	Y		4	72 GB	3.4%	Y

Table 1: Traffic composition of common LLMs with different parallelism and whether the traffic is carried in the network.

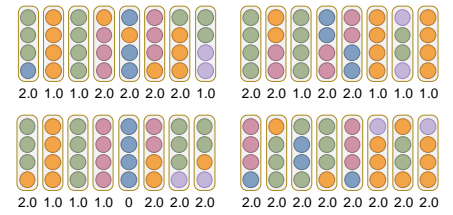
across jobs competes in the network. To minimize network congestion, we focus on managing DP traffic.

DP replicates the model across GPUs, with each GPU processing a different data batch. Fully Sharded Data Parallelism (FSDP) extends DP by sharding parameters across GPUs. Both require synchronizing gradients or parameters at the end of each training iteration through collective communication. These collectives generate traffic proportional to model size with the same volume and pattern, so we treat them identically and refer to both as DP traffic. When combined with other parallelisms such as PP and TP, only a subset of GPUs shares the same model replica; we call this subset a *replica group*, and each performs its own collective independently.

Ring-based collectives. We focus on ring-based collective algorithms, which are bandwidth-optimal and generate the sparsest traffic pattern [60]. When a replica group spans multiple racks, each ToR generates one flow entering and leaving, regardless of how many workers reside in that rack or their ordering. We refer to such traffic as DP-flows throughout the rest of the paper. This sparsity fundamentally changes the property of congestion-free states in shared GPU clusters.

3.1 Congestion-Free States are Achievable

Consider again the example in Figure 2, now with GPU jobs. We assume each server has one GPU and runs training with DP-only (i.e., one replica group per job); we discuss the multi-GPU and hybrid parallelism cases in Section 5.3. Since DP traffic dominates network congestion, we analyze only DP synchronization traffic, where each GPU sends one unit of demand to its neighboring node. The total network demand

**Figure 3: Sample congestion-free states for GPU clusters, for jobs shown in Figure 2.** Despite different placements, all states have two or fewer fragmented jobs, thereby generating at most two units of demand per rack.

generated by each job is the same across CPU and GPU jobs; however, unlike the CPU case, the traffic matrix is *sparse*: ring-based collectives generate exactly one flow per ToR per fragmented job. As long as each ToR contains fewer than two fragmented jobs, the number of outgoing flows stays below the number of uplinks.

This sparsity resolves the ill-defined optimization problem from Section 2.2. In particular, there exist states in which the traffic leaving each ToR does not exceed its uplink capacity (bottom-left of Figure 2). We define such states as *congestion-free*, since this condition allows each DP flow to be assigned a dedicated uplink, achieving *path isolation*. Under minimal uplink provisioning, such states always exist (§5.1). For CPU workloads, operators must balance network contention against migration overhead [28, 32, 33]. In contrast, for ML workloads this tradeoff disappears: because congestion-free states are always attainable, they can be enforced as a constraint, allowing the optimization to focus solely on minimizing migrations.

Now, we turn to minimizing migrations: given a contended state, what is the minimum number of worker movements to reach any congestion-free state? The bottom of Figure 2 shows such placement with the minimum amount of migration, requiring only 4 compared to 11 in the CPU case. Such a reduction stems from another property of GPU jobs: congestion-free placements are readily available.

3.2 Congestion-Free States Are Abundant

The achievable nature of congestion-free states implies another useful property: *any* state where the number of flows leaving each ToR does not exceed its uplink count is equally good, and we do not need to find a single optimal arrangement. For instance, Figure 3 shows four other congestion-free placements for GPU workloads, in addition to the bottom right placement in Figure 2. Notice that even seemingly fragmented placements, like the bottom-right one, are congestion-free.

This flexibility compounds in several ways. First, workers within a replica group are order-insensitive: they form a ring in any order through a simple re-assignment of ranks for

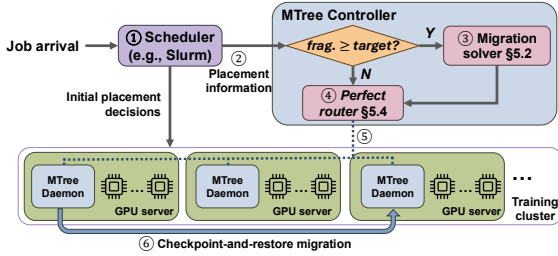


Figure 4: Overview of MonkeyTree. A centralized controller and per-node daemons operate alongside existing schedulers.

communication, and still produce the same sparse traffic pattern in the network. Second, the constraint is local to each ToR, as satisfying the uplink bound at one ToR is independent of other ToRs. Consequently, unlike CPU workloads, where low-congestion placements are rare and expensive to reach, congestion-free states in a shared GPU cluster are plentiful. Hence, we can always reach one from any contended state through a small number of migrations (§6).

3.3 Congestion-Free States are Self-Reinforcing

Once a cluster reaches a congestion-free state, maintaining it requires only incremental effort. A single new job spans a limited number of ToRs, so its arrival can violate the uplink constraint at only those few racks—a small, localized perturbation to an otherwise valid configuration. Because valid placements are abundant, restoring compliance never requires a far-reaching search: a small number of migrations among the affected racks suffices. This creates a virtuous cycle: few migrations mean low overhead, low overhead makes proactive maintenance practical, and a well-maintained cluster presents only simple, local violations to correct. Rather than gradually drifting into a highly contended state that demands expensive cluster-wide reorganization, the system naturally remains in the neighborhood of valid configurations.

4 MONKEYTREE SYSTEM DESIGN

Our analysis in Section 3 shows that migration in shared GPU clusters is both practical and desirable. We introduce MonkeyTree, a system that eliminates network contention in shared GPU clusters through migration-based defragmentation.

Overview. Figure 4 illustrates MonkeyTree’s architecture and workflow. The system consists of a centralized controller (§4.1) and distributed daemons (§4.2), operating alongside existing job schedulers without modifying their placement logic.

The workflow begins when a job arrives, and the existing job scheduler ① assigns GPU placements to the new job. Rather than intervening in placement decisions, MonkeyTree monitors the resulting cluster state ② and initiates migration

only when necessary. We set a fragmentation threshold based on the ToR uplink count to ensure path isolation is always achievable (§5.1). If any rack exceeds this threshold, the controller invokes the migration solver ③ to compute the minimum worker movements needed to restore a congestion-free state (§5.2). Whether or not migrations are needed, the controller computes routes ④ that provide path isolation for all DP flows (§5.4). It then sends migration instructions and routing assignments to the daemons ⑤. Each daemon executes its assigned migrations via an efficient checkpoint-and-restore operation ⑥ and configures local routing rules to steer DP traffic onto isolated paths.

4.1 MonkeyTree Controller

The controller interfaces with the cluster’s job scheduler (e.g., Slurm [31]) to observe placement decisions. It does not modify the scheduler’s allocation logic, but allows the scheduler to make an initial decision after job arrival. If the placement decision violates the fragmentation constraint, MonkeyTree intervenes and computes a new placement that satisfies the constraint while minimizing migrations.

Migration decisions. When a new job’s placement causes any rack’s fragmentation to exceed the threshold, the controller computes the minimum migrations to restore compliance. The threshold is set to equal the number of uplinks per ToR, ensuring that path isolation is always achievable. Section 5 details the migration algorithm.

Perfect routing solver. After each job arrival or migration, the controller reconfigures routing to achieve path isolation. MonkeyTree uses a deterministic routing scheme, called *Perfect routing*, that assigns each DP traffic a dedicated uplink, guaranteed to exist as long as fragmentation stays within the threshold. The controller transmits routing assignments to the daemons, which compute ECMP hashes that steer traffic onto the assigned paths, similar to prior work [9, 38].

4.2 MonkeyTree Daemons

Daemons run on each server and handle job lifecycle operations: launching jobs with pre-computed ring orderings, executing migrations, and updating routing configurations.

Migration execution. We implement migration itself as checkpoint-and-restore over GPUDirect RDMA. When the controller initiates a migration, the source daemon pauses training after the current iteration completes and checkpoints model state to the destination. The destination daemon receives the checkpoint into CPU memory, then loads it onto GPUs and resumes training with the replica group. This approach leverages existing checkpointing infrastructure and avoids overwhelming GPU memory during transfers. Section 7 describes our prototype implementation.

$w_0(s, t)$	Initial placement: # of job s workers on ToR t
λ	Fragmentation threshold
Input	$S = \{s_0, \dots, s_J\}$ Set of jobs to be placed, where job j requires s_j workers
T	Number of ToRs (racks)
C	ToR capacity, i.e., number of nodes below a ToR
Output	$w(s, t)$ Final placement: # of job s workers on ToR t

Table 2: Variable definitions.

5 MONKEYTREE FORMULATION

In this section, we first show that for a GPU cluster with at least two uplinks per ToR, congestion-free states are well-defined and always achievable (§5.1). We then formulate the problem of minimizing the number of migrations to bound the number of DP-flows that enter the fabric as an Integer Linear Program (ILP) (§5.2, §5.3). Finally, we present a routing scheme, *Perfect routing*, that exploits the bound on DP-flows to guarantee path isolation, nearly eliminating congestion (§5.4).

5.1 Bounding Fragmentation Degree

Formally, we define a rack's *fragmentation degree* as the number of DP flows originating from this rack that have destinations outside it. For pure DP jobs, this equals the number of fragmented jobs under the rack. We begin by characterizing what is achievable given a cluster and a set of jobs.

THEOREM 1. *For any cluster and any set of pure DP or FSDP jobs running on it, there exists a job placement such that no rack has a fragmentation degree greater than two.*

Proof. Order the jobs arbitrarily, and place their workers sequentially across the cluster from left to right. For any rack, this placement induces at most three contiguous regions. The front consists of the trailing workers of a job that began on a previous rack and finishes on the current one. The end consists of the leading workers of a job, with the remaining workers placed on subsequent racks. The middle consists of jobs that are entirely contained within the rack. Jobs in the middle region do not contribute to fragmentation, since all of their communication remains local to the rack. Moreover, the front and end regions each contain at most one job that spans racks. Therefore, each rack can contain at most two fragmented jobs, implying that the fragmentation degree of any rack is at most two.

We note that there are scenarios in which achieving a fragmentation degree better than two is impossible. For example, consider two jobs whose sizes each exceed the capacity of a single rack, running on a cluster with three racks. In this case, the two jobs must overlap on at least one rack, forcing that rack to have a fragmentation degree of at least two.

Once a placement limits the number of DP-flows exiting each rack to be less than the number of ToR uplinks, a congestion-free cluster only requires a *routing scheme* that

$$\min \sum_{\text{all } s, t} \frac{1}{2} |w(s, t) - w_0(s, t)| \quad (1)$$

$$\text{s.t. } \sum_{t < T} w(s, t) = s_j \quad \forall \text{ Job } j \quad (2)$$

$$\sum_{s \in |S|} w(s, t) \leq C \quad \forall \text{ ToR } t \quad (3)$$

$$|\{s : w(s, t) > 0 \text{ and } \sum_{t' \neq t} w(s, t') > 0\}| \leq \lambda \quad \forall \text{ ToR } t \quad (4)$$

$$w(s, t) \geq 0 \quad \forall s, t \quad (5)$$

Listing 1: MonkeyTree's ILP formulation for minimizing migration.

assigns each flow to a dedicated uplink, guaranteeing path isolation. We derive such a routing scheme, which we call *Perfect routing*, for a two-tier network topology, detailed in Section 5.4. Combined with the worst-case minimum fragmentation degree of two, our routing scheme implies that provisioning just two uplinks per rack is sufficient for a congestion-free network for shared GPU clusters.

The above arguments establish that a congestion-free state is *achievable*. Next, we formulate MonkeyTree's core algorithm that finds a sufficiently defragmented placement from an initial fragmented one, minimizing the number of migrations between the two. We assume each rack has more than two allocated uplinks and aim to find a congestion-free state in which no rack's fragmentation degree exceeds the number of uplinks.

5.2 MonkeyTree ILP for DP and FSDP Jobs

In this section, we identify the minimum number of migrations needed to defragment every rack below a set threshold, thereby achieving a nearly congestion-free state. We focus on pure DP and FSDP jobs here, and extend our formulation to model parallelism in Section 5.3.

Table 2 defines the variables we use in this formulation, and Listing 1 illustrates MonkeyTree's optimization problem. We model this problem as follows: let S denote the set of jobs, and let T denote the number of racks. We construct a bipartite graph in which the left nodes $s \in S$ correspond to fragmented jobs in the cluster, and the right nodes t ($0 \leq t < T$) correspond to the racks. For every pair (s, t) , we introduce an edge whose weight $w(s, t)$ denotes the number of workers of job s currently placed on rack t . Let $w_0(s, t)$ denote the initial worker placement. The resulting optimization objective is thus Equation 1 in Listing 1, capturing the total number of worker migrations as the ℓ_1 distance between the initial and final assignments.

For the constraints, Equations 2 ensure that each job is fully assigned, while Equation 3 ensures that each rack receives fewer jobs than its capacity. The key constraint is Equation 4: the left-hand side constructs a set of fragmented jobs on each rack t . The first part of the set construction checks whether rack t contains job s , while the second checks whether job s is fragmented. Hence, the cardinality of this set is the number of fragmented jobs, which were required to be at most λ

(RHS). Satisfying this constraint guarantees that the resulting placement is sufficiently defragmented to meet the routing requirements for a congestion-free state.

This optimization problem is a variant of the sparsity constrained transport problem, which is NP-hard [10]. In practice, we transform it into an integer linear programming (ILP), which surprisingly has a practical solve time. For example, for clusters with up to 1,024 GPUs, solve times are on average under one second (Section 6.5).

We attribute this efficiency to the ability of branch-and-bound solvers [35] to exploit the abundance of the solution space. To build intuition for the runtime, let γ denote the number of migrations in searching for a solution. The number of distinct cluster states reachable within γ moves is $O(N^{2\gamma})$, where N is the cluster size. As branch-and-bound progressively discovers feasible solutions with increasing migration counts, large portions of the search space are pruned, since the solver discards solutions requiring the same or more moves. We believe that, because the optimal number of migrations is typically small (§6.5), the solver explores a limited effective search space, resulting in fast ILP solving time.

5.3 Extending to Model Parallel Jobs

The prior formulation works for DP and FSDP jobs but fails to capture additional complexities introduced by model parallelisms. We address additional parallelisms in turn.

Pipeline parallelism (PP). Pipeline parallelism shards the model between layers into distinct stages that run on separate GPUs. Activations are communicated point-to-point between stages. Data-parallel replicas are thus across each stage, and the subsequent all-reduce (DP-flows) only happens within these stages. We only use our *Perfect routing* algorithm to load balance pipeline traffic and ignore accommodating them in our formulation, because they are small (§3) and therefore have little impact on end-to-end job completion time. Instead, we update our formulation to treat pipeline stages as independent jobs, thereby controlling each stage’s DP-flow separately.

Tensor parallelism (TP). Tensor parallelism shards an individual layer of a DNN across GPUs, resulting in substantial communication volume. For this reason, the standard practice confines TP *within* a single server, where GPUs communicate over high-bandwidth interconnects such as NVLink [43, 48].

Each TP shard forms an independent DP replica group and produces its own all-reduce traffic. As a result, a fragmented job that previously generated a single ring per rack now produces as many DP-flows as there are GPUs per server when TP is employed. Following the standard configuration of 8 GPUs per server [18, 43], we assume a maximum TP degree of 8 throughout this paper, yielding up to 8 independent DP flows per fragmented job per rack. We now generalize our previous result on the attainable fragmentation degree

for TP jobs. Let d_s denote the TP degree of job s , and let $D_C = \max_{\{s \in S\}} d_s$ represent the maximum TP degree across a set of jobs. Then, the maximum number of DP-flows per server is D_C , and we have the following result:

COROLLARY 1. *For any cluster with ML jobs, with maximum TP degree of D_C , there exists a job placement such that no rack has a fragmentation degree greater than $2D_C$.*

The proof follows directly from the argument in Theorem 1, with each fragmented job now generating up to D_C DP-flows. As a consequence, under standard tensor-parallel configurations with eight GPUs per server, avoiding congestion requires provisioning at least 16 uplinks per rack. We then refine the fragmentation constraint in Listing 1 (Equation 4) to weigh the contribution of each job s by the number of rings it produces d_s . **Expert parallelism (EP).** In MoE models, each layer contains multiple expert sub-networks, only a subset of which activate for any given token. Expert parallelism (EP) places each expert on a different GPU. Between layers, an *all-to-all collective* dispatches tokens to their assigned experts. Another all-to-all collective then combines the results, generating communication across all participating GPUs. Without replicating experts across GPUs, EP generates all-to-all traffic on par with DP, violating MonkeyTree’s assumption where sparse DP traffic dominates. While defragmentation continues to benefit EP workloads, MonkeyTree cannot guarantee congestion-free execution. We discuss this limitation and potential extensions in §8.

5.4 Perfect Routing

In this section, we describe the *Perfect routing* algorithm, which exploits our bound on the number of DP-flows entering the fabric to guarantee path isolation for them. For other mice flows such as pipeline parallel traffic, *Perfect routing* load balances them via round robin across available spines.

To route DP-flows, we model the problem as a bipartite edge-coloring instance. Each vertex on the left and right corresponds to a ToR switch, and for every flow between two distinct ToRs, we introduce an edge connecting the corresponding vertices. The objective is to assign a color to each edge, such that no two edges incident to the same vertex share a color. Here, each color corresponds to a distinct flow-to-uplink assignment.

We compute such a coloring in polynomial time by reducing the problem to bipartite matching, and solve it using the Hopcroft–Karp algorithm [26]. The number of colors required equals to the maximum number of flows sent or received by any rack, which is always less than the number of uplinks in MonkeyTree.

We note that when *Perfect routing* executes separately on a fragmented cluster without migration, the number of required colors can exceed the number of physical uplinks per ToR. In these cases, we collapse multiple colors (flows) onto the available uplinks in a round-robin fashion to evenly

Model	DP	FSDP	TP	PP
GPT3-13B [43]	✓	✗	✗	✗
GPT3-7B [43]	✓	✗	✗	✗
GPT-OSS-120B [49]	✗	✓	✗	✗
GPT-OSS-20B [50]	✗	✓	✗	✗
Llama2-70B [39]	✓	✓	✓	✓
Llama3-70B [40]	✓	✓	✓	✓

Table 3: Jobs and parallelization strategies to generate traces.

distribute load, multiplexing multiple flows onto the same path. We evaluate *Perfect routing* without MonkeyTree’s defragmentation in Section 6 to isolate the performance impact of routing alone.

6 EVALUATION

We evaluate MonkeyTree in large-scale simulations and compare its performance with that of state-of-the-art algorithms for mitigating ML training congestion. In §6.1 we describe the setup and parameters for our experiments, as well as compared schemes. §6.2 evaluates MonkeyTree’s ability to provide isolation between competing jobs and compares that to the performance of other algorithms. §6.3 zooms in on a few specific traces to study how fragmentation and network load change over time for various systems. §6.4 presents results on the impact of uplink provisioning on system performance. §6.5 analyzes how many migrations MonkeyTree performs and the ILP’s solving time. In §6.6, we discuss the migration overhead cost to job performance. Finally, §6.7 studies the impact of the migration threshold on the number of migrations.

6.1 Simulator Setup

MonkeyTree Simulator. To evaluate MonkeyTree on large-scale topologies, we build a custom Rust simulator for multi-tenant distributed ML training in ~20k lines of code. For the network backend, we use a standard maxmin flow-level simulator [6]. Our simulator represents individual training jobs as graphs of compute and communication steps, similar to prior work [66, 68]. To get concrete values for the computation steps, we use the estimation techniques found in [65].

Job Selection. Table 3 presents the jobs we use in our simulation, along with the parallelization strategies available for selection. We generate job traces by randomly selecting jobs, determining which parallelization strategies to apply, and specifying the degree of each parallelization.

Traces. We generate traces of job arrivals by modeling the system as a Poisson arrival process across a series of load levels from 50% to 100%. We plot the resulting slowdown for several systems in Figure 5.

Slowdown definition. In several experiments, we plot the *slowdown* in job completion. We define this slowdown as the division of the actual job runtime by its ideal completion time.

Topology. We use a standard two-tier spine tree topology, where hosts are connected to ToR switches, and these in turn are connected to a spine layer of switches. Unless otherwise specified, we place 8 hosts below each ToR, each equipped with 8 GPUs, and each GPU is given its own 400 Gbps NIC. The oversubscription ratio changes across experiments.

Cluster scheduler. We use a locality-aware job scheduler similar to Slurm [31]. It first checks if any rack can fully accommodate the job it is scheduling. If it can, it will place it on the rack with the fewest available hosts. Otherwise, it finds the rack with the most available hosts, assigns as much of the job as possible to those hosts, and then recursively calls itself with the remaining workers to be scheduled.

Migration simulation. To simulate the overhead associated with migration, we implement a 4-step process. First, before migrating, jobs must synchronize at the iteration barrier. Secondly, to model the movement of the model weights, the migrating GPUs transfer their model shard as a flow from their GPU to the destination. Thirdly, migration does not complete until the destination GPU is free of any workers that were running on it. Finally, after all workers have reached their destination, we pause resumption for 10 seconds to model re-initialization overhead, based on our testbed measurements (§7).

Simulated algorithms. We simulate several approaches to mitigate congestion in multi-tenant training clusters:

- **MonkeyTree.** We run the MonkeyTree system as described in Figure 4. On every job arrival, MonkeyTree controller monitors the fragmentation of each rack and intervenes if the set threshold is exceeded. In our experiments, we typically set the threshold to the number of uplinks per ToR. To study the benefit of migration alone, we also run variations of MonkeyTree built on top of ECMP and Crux, rather than *Perfect routing*.
- **ECMP** [27]. ECMP is a classic load-balancing scheme that hashes the 5-tuple of flow information at each switch. This results in flows being pseudorandomly spread across the available paths.
- **Crux** [9]. Crux is a greedy routing scheme that orders jobs by expected GPU utilization and routes them one at a time to minimize overlap.
- **Perfect-routing-only** (§5.4). We evaluate the *Perfect routing* algorithm without MonkeyTree’s migration as a separate baseline to isolate the performance impact of routing and migration.
- **SGLB** [53]. SGLB is a load-balancing scheme for AI clusters in which each switch dynamically routes flows away from congested paths. Switches communicate congestion information between each other to achieve rapid convergence.
- **Full bisection with packet spraying**. Finally, we also simulate a version of the cluster provisioned with a full-bisection fabric and packet spraying enabled, representing the performance upperbound at a high cost.

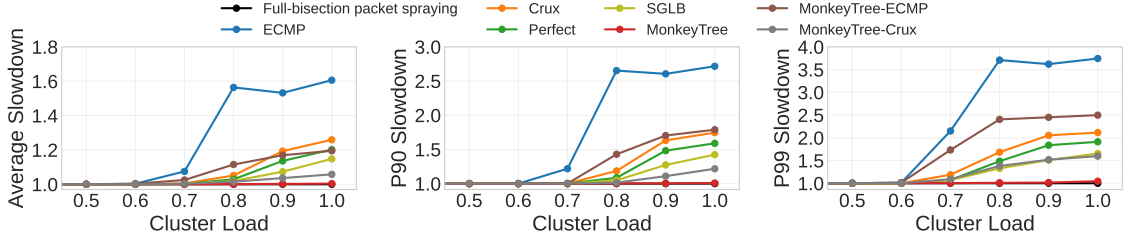


Figure 5: Average, p90, and p99 job completion slowdown under varying cluster load for a 1,024-GPU cluster. MonkeyTree’s migration-based approach reduces p99 slowdown by up to 3.59× compared to routing-only schemes.

6.2 Performance Under Varying Cluster Load

We begin our evaluations by comparing the performance of various algorithms of jobs running in a shared cluster. Figure 5 presents the average, p90, and p99 job completion slowdowns for job traces of varying load on the x-axis, with different algorithms. The y-axis shows the slowdown. The cluster comprises 1,024 GPUs, with 64 GPUs and 16 uplinks per rack.

Under the highest load, MonkeyTree maintains a nearly contention-free state, having only a 4% slowdown at the 99th percentile. On average, it performs within 0.5% of the packet-spraying baseline. This slowdown is due to migration overhead and brief congestion during pipeline-parallel transfers.

For different routing algorithms, our *Perfect routing* algorithm guarantees path isolation when possible and load-balances otherwise. On the other hand, ECMP suffers from hash collisions, leading to elephant flows being routed together, while Crux’s greedy heuristic occasionally fails to provide path isolation even when it is possible to do so. Notably, *Perfect-routing*-only outperforms ECMP and Crux, beating Crux by up to 5% on average. SGLB is the best of the non-MonkeyTree baselines, as its dynamic rerouting enables finer-grained sharing of available links. MonkeyTree beats all of these routing-only approaches by 1.58× to 3.59× in p99 job completion time.

We demonstrate the benefit of migration by evaluating MonkeyTree-variants with migration only (without the *Perfect routing* algorithm). Notably, MonkeyTree-ECMP outperforms Crux by 5% and matches *Perfect-routing* at the highest load. At high load, fragmentation generates significant network contention that no routing scheme, however sophisticated, can fully resolve. MonkeyTree addresses the problem at its root: by migrating jobs to reduce fragmentation, even a simple scheme like ECMP is sufficient to outperform more intelligent routing-only approaches. Compared to their corresponding baselines, MonkeyTree-Crux improves slowdown by up to 32% over Crux, while MonkeyTree-ECMP attains up to a 1.5× speedup over ECMP.

6.3 Fragmentation Evolution Over Time

Figure 6 plots the cluster-wide and per-rack maximum fragmentation over time for ECMP, Crux, and MonkeyTree on a 1,024-GPU cluster with three uplinks per rack, using pure DP/FSDP job traces at 70% to 100% load. The top row shows the total number of fragmented DP replica groups; the bottom row shows the maximum number of DP flows (rings) per ToR, with values exceeding 3 indicating congestion.

At 70% load, fragmentation remains near zero except for two brief bursts, with little difference among algorithms—the cluster scheduler alone suffices. At 80% load, ECMP suffers high fragmentation due to an early burst of arrivals, while MonkeyTree and Crux (overlapping in the Figure) escape by completing jobs faster.

At 90% load, the arrival rate overwhelms the cluster scheduler and routing-only schemes. ECMP and Crux reach average fragmentation degrees of 86 and 77, respectively, after the first 50 hours; Crux is slightly better because its more even traffic spreading completes jobs faster, freeing slots for better placement decisions. MonkeyTree reduces total fragmentation by 4.85× over Crux, only once exceeding 40 fragmentation degrees, and maintains per-rack fragmentation at or below 3—within *Perfect routing*’s path-isolation guarantee. This enables MonkeyTree to finish 1.25× faster than Crux and 1.7× faster than ECMP.

Finally, at 100% load, ECMP and Crux become nearly indistinguishable, differing by an average of just 3 fragmentation degrees. MonkeyTree oscillates between 3 and 4 per-rack fragmentation as it continuously defragments to keep pace with demand, finishing 1.33× faster than Crux.

6.4 Performance across Oversub. Ratios

By keeping fragmentation in check, MonkeyTree requires only a minimum number of uplinks, twice the number of DP flows per job, to guarantee path isolation. This implies MonkeyTree’s performance is solely determined by the number of uplinks per ToR, thereby enabling higher oversubscription than conventional routing-based approaches.

Figure 7 presents heatmaps of average and p99 slowdown for MonkeyTree, Crux, ECMP, Perfect routing, and SGLB

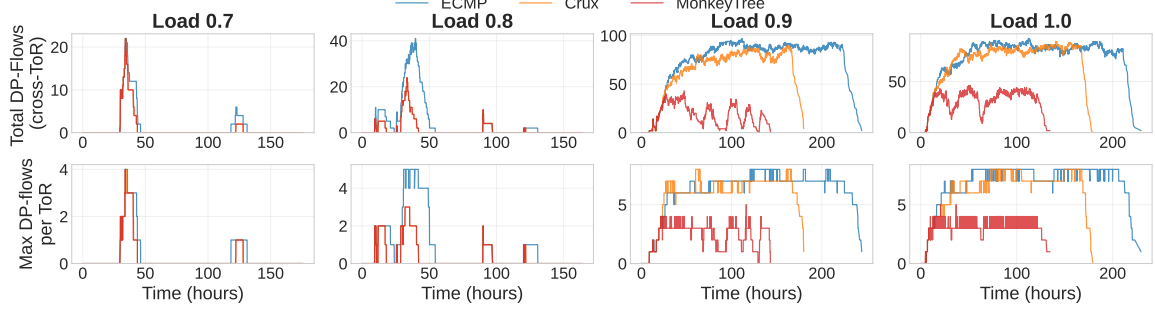


Figure 6: Cluster-wide and per-rack fragmentation over time at 70–100% load in a 1,024-GPU cluster. MonkeyTree’s active defragmentation keeps per-rack congestion within isolable bounds and yields up to 1.7× faster job completion than routing-only schemes.



Figure 7: Heatmaps of average and p99 slowdown across oversubscription ratios for a 2,048-GPU cluster for different systems. MonkeyTree achieves near-optimal performance at 16:1 oversubscription while competing schemes require up to 4× more uplinks to match.

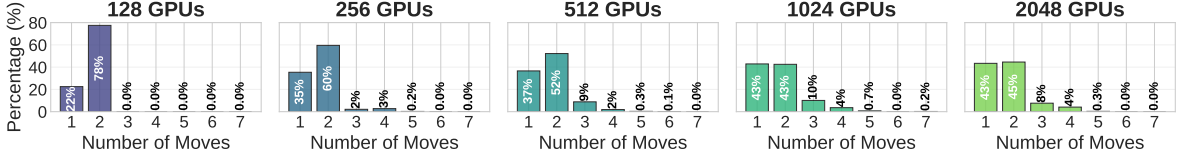


Figure 8: Distribution of job migrations required to restore low fragmentation across cluster sizes. Over 80% of defragmentation events require only one or two moves, and the average remains below 2 regardless of scale.

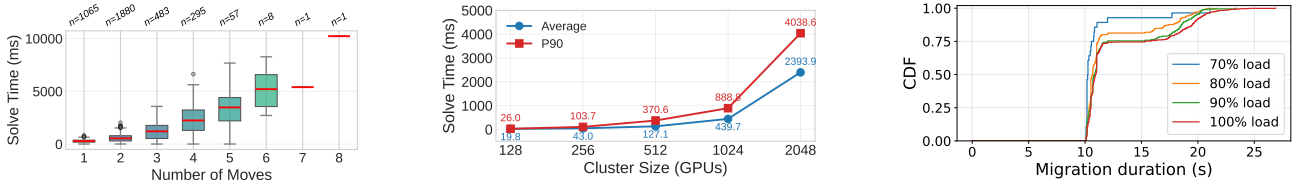


Figure 9: ILP solve time vs. number of migrations on a 1,024-GPU cluster. Runtime scales with move count, averaging 540 ms in the common two-move case.

Figure 10: ILP solve time across cluster sizes from 128 to 2,048 GPUs. p90 solve time stays under 5 s at 2,048 GPUs, well within practical planning budgets.

Figure 11: CDF of migration duration at different loads. We assume 10 seconds of system overhead. Remaining time is due to network transfers and iteration synchronization.

across a 2,048-GPU cluster. The y -axis varies the number of GPUs per rack from 16 to 256, and the x -axis varies the number of uplinks per rack by scaling the spine count until

reaching full bisection bandwidth (entries along the diagonal). Packet spraying with full bisection bandwidth (not plotted)

achieves a slowdown of 1 along this diagonal and serves as the baseline.

MonkeyTree attains p99 performance within 5% of packet spraying at an oversubscription ratio of 16:1, with average slowdown below 0.3% regardless of how many additional links are provisioned. Its only requirement is that the minimum number of uplinks is present; beyond that, it is nearly agnostic to the oversubscription ratio. Other systems require substantially more bandwidth. At 256 GPUs per rack, SGLB, the best competing scheme, needs 4 \times the uplinks to match MonkeyTree's p99 performance. ECMP performs worst, with an average slowdown of up to 50% even at full bisection.

Notably, competing schemes do not maintain consistent performance even at a fixed oversubscription ratio. Crux, for instance, has a 10% p99 slowdown at 4:1 oversubscription with 256 GPUs per rack but 27% at the same ratio with 128 GPUs per rack. This is because the oversubscription ratio alone does not determine performance: at a fixed cluster size, fewer GPUs per rack means more racks, which causes more jobs to span rack boundaries and increases fragmentation. At the same time, each rack has fewer uplinks to absorb this fragmentation. Hence, what determines routing performance is the combination of fragmentation and oversubscription ratio. By controlling fragmentation, MonkeyTree is the only system whose performance depends solely on the number of uplinks.

6.5 Migration Solver Scalability

We evaluate the efficiency of MonkeyTree's ILP solver, examining the number of migrations required to defragment the cluster and the solver's runtime characteristics. These results are critical for establishing that MonkeyTree's migration planning is lightweight enough to be invoked frequently in practice.

Figure 8 presents the distribution of required job migration (number of moves) to lower the fragmentation below two on clusters of varying sizes across five traces each. The distribution shifts as cluster size increases, but the average remains consistently between 1.7 and 1.8. Approximately 80% of the weight is concentrated on one or two moves across all scenarios, and move counts greater than 5 are rare, occurring in fewer than 1% of the migrations for each cluster.

Figure 9 shows the distribution of the ILP's solve time versus the number of moves across five traces on a 1,024-GPU cluster. The most common case of two moves averages 540 ms and never exceeds 4 s. Solve time scales roughly linearly with the number of moves, reaching 6.7 s at 6 moves. Cases requiring 7 or 8 moves each occurred only once and are thus not statistically meaningful. Overall, these results confirm that the ILP's runtime is governed primarily by the number of moves (§5.2).

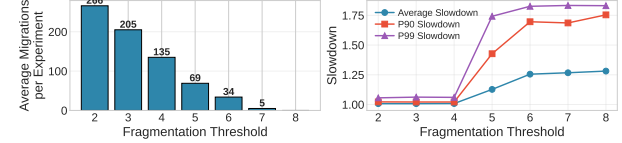


Figure 12: Number of migrations and job slowdown vs. fragmentation threshold on a 1,024-GPU cluster. A threshold matching the number of uplinks achieves near-optimal performance with diminishing returns from further reduction.

Finally, Figure 10 plots the ILP's solve time across cluster sizes ranging from 128 to 2,048 GPUs. For clusters of 1,024 GPUs or fewer, the average solve time remains under 0.5 s with a p90 below 1 s. At 2,048 GPUs, solve time increases by over 5 \times , with an average of 2.39 s and a p90 of 4.04 s. Even so, this remains well within practical limits: migrations are triggered infrequently and can tolerate seconds of planning latency, making the ILP viable even at the large cluster sizes.

6.6 Migration Overhead

This section analyzes the overhead incurred by migration to keep fragmentation below the threshold. Figure 11 presents CDFs of migration duration across traces on a 1,024-GPU cluster at 70% to 100% load. All distributions start at 10 seconds, reflecting the baseline latency for workers to resume after migration completes.

Across all loads, the median migration duration remains below 11 seconds, indicating that most migrations add little overhead beyond the baseline latency. The longest observed migration takes 26.89 seconds; these tail cases arise from dependency chains in which a job must wait for downstream migrations to complete before it occupies the target slot. Even so, within 30 seconds of initiating migrations, the cluster is fully restored to a congestion-free state.

The per-job overhead is also modest. No job in our experiments is migrated more than 6 times over its lifetime, resulting in a worst-case downtime of 115 seconds. Compared to that job's ideal runtime of 5.34 hours, migration constitutes less than 0.6% overhead.

6.7 Threshold Sensitivity

Section 5.1 established that a per-rack fragmentation degree at or below the number of uplinks suffices for Perfect routing to guarantee path isolation, and that a fragmentation degree of two is always feasible. The fragmentation threshold controls when MonkeyTree triggers migrations: MonkeyTree migrates jobs only when a rack's fragmentation exceeds this threshold. Setting it above the number of uplinks reduces migrations at the cost of additional congestion. This section evaluates the tradeoff between this threshold and the resulting migration

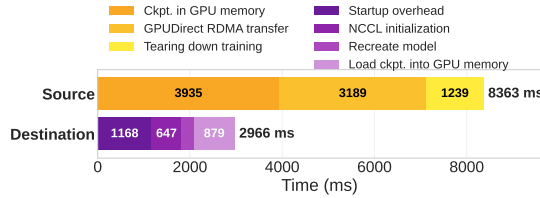


Figure 13: Timing breakdown of migrating a single Llama3-8B worker on the testbed. Checkpoint composition dominates at 3.93 s, and system overhead besides network transfer is 9.02 s, validating the 10 s migration budget assumed in simulation.

count and slowdown, using a trace of 1.2k pure DP and FSDP jobs on a 1,024-GPU cluster with four spine switches.

Figure 12 plots the number of migrations alongside the average, p90, and p99 slowdown. At a threshold of 4, matching the number of uplinks, p99 slowdown is within 6% of ideal, and the average is within 1%. This is slightly worse than the results in §6.2, as a workload composed entirely of FSDP and DP jobs with few uplinks presents a more constrained setting than the full workload mix. Decreasing the threshold below four yields less than 0.5% additional improvement: *Perfect routing* already guarantees path isolation at a fragmentation threshold of four, so further migrations cannot eliminate elephant-flow collisions. A lower threshold only reduces collisions between elephant flows and in-flight migration traffic, yielding a marginal benefit offset at the cost of up to 2× more migrations.

7 MONKEYTREE PROTOTYPE

We prototype MonkeyTree on a testbed of five servers, each with one Nvidia A100 GPU [1] and 100 Gbps ConnectX-5 NIC [44], to demonstrate practicality and quantify migration overhead.

RDMA-Based Checkpointing. We extend PyTorch’s Distributed Checkpoint (DCP) [52] with custom StorageReader and StorageWriter interfaces that perform RDMA transfers instead of filesystem I/O for migration. During migration, the source worker writes GPU tensors directly to the CPU DRAM of a remote staging server using GPUDirect RDMA. Targeting CPU DRAM avoids contention for GPU memory at the destination and enables pipelined loading, allowing tensor transfers to overlap with model initialization. The replacement worker constructs ShardedTensor templates matching the original layout and accepts RDMA writes to retrieve the checkpoint. A lightweight signaling protocol coordinates shard availability without blocking the critical path.

Each MonkeyTree daemon creates a migration listener at cluster start with a pre-allocated buffer to hold the checkpoint. When the controller triggers a migration, it sends the migrating job a signal with the worker that is migrating and its destination.

The daemons on the migrating jobs wait for the current training iteration to complete before initiating the RDMA checkpoint. Once the transfer finishes, the job synchronizes, loads from the checkpoint, and resumes training.

Prototype microbenchmark. Figure 13 presents the timing breakdown of migrating a single worker in a 4-node Llama3-8B training instance using our prototype. The top column plots overhead on the sender side (source of migration), while the bottom one plots the receiver side (destination of migration). The dominant cost is composing the checkpoint at 3.93 s. MonkeyTree-daemon transfers the 12 GB checkpoint shard (model weights and optimizer state) over RDMA in 3.19 s end-to-end. The transfer itself accounts for only 1.07 s at 90 Gbps; the remainder is serialization and memory management overhead. Source server cleanup adds 1.24 s, though this does not block the migrated model from resuming. On the destination, NCCL initialization, model loading, and other startup costs total 2.97 s. Excluding the RDMA transfer’s network time, the total overhead is 9.02 s, validating the 10 s migration budget excluding RDMA transfer assumed in simulations.

8 DISCUSSION

Scaling MonkeyTree to larger clusters. MonkeyTree’s ILP exhibits p90 solve times below five seconds for clusters of up to 2048 GPUs. We divide larger clusters into independent partitions, each managed by an independent MonkeyTree controller, keeping ILP solve times tractable. A second-tier MonkeyTree controller then treats each sub-cluster as a virtual rack and manages migrations across them.

Extending to three-tier topologies. The partitioning strategy above enables a natural extension to three-tier (or deeper) topologies: the second-tier MonkeyTree controller manages fragmentation beyond the spine switches. Furthermore, an extension of Theorem 1 shows that if no single job exceeds the bounds of a partition, then 1 is achievable for cross-partition fragmentation. Therefore, only one uplink per partition is necessary. This keeps the routing problem polynomial, enabling a straightforward extension of Perfect routing to three-tier topologies. We leave the performance evaluation of this scheme to future work.

Rail topologies. A rail-optimized topology equips servers with multiple NICs, each connected to a disjoint leaf switch (the rail), so that parallel communication streams do not interfere [45, 54]. MonkeyTree is compatible with these networks by reasoning about fragmentation across rails rather than racks, allowing each rail to sustain higher oversubscription ratios without sacrificing performance.

Limitations of MonkeyTree on EP and CP. Our current formulation assumes that collective traffic is dominated by data parallelism, which does not hold under all parallelism

strategies. First, expert parallelism (EP) without expert replication introduces all-to-all traffic that scales with top- k gating, MoE layer count, model dimension, and batch size, potentially rivaling DP traffic volume. Models with modest top- k gates and expert count (e.g., Llama-4 Scout) remain tractable, as their EP traffic resembles pipeline traffic in volume. When experts are replicated across DP groups, all-to-all narrows to a confined many-to-many pattern.

Second, context parallelism (CP) partitions long input sequences into contiguous segments, which are processed in parallel across workers, coordinating cross-segment attention through collective communication. Under CP, every node participates in two separate rings: one for data-parallel groups and one for context-parallel groups. This transforms the placement problem into an NP-hard variant of the min-cut problem. While our ILP can be extended to handle both EP and CP, we do not offer congestion-free guarantees. We leave EP-aware topology optimization under varying replication strategies and the evaluation of CP-aware placement to future work.

9 RELATED WORK

Mitigating congestion in multi-tenant training clusters. Prior work on scheduling multi-tenant training jobs follows two directions. The first temporally shares network links by interleaving communication from competing jobs into idle periods during computation [55–57]. This approach relies on favorable computation-communication overlap patterns, which are not always present. The second spatially distributes traffic across multiple paths via routing or adaptive load balancing [9, 53]. MonkeyTree employs similar load-balancing mechanisms but also controls fragmentation to bound aggregate network load. More recent systems combine temporal and spatial techniques [59, 73]; however, none provide explicit guarantees on maximum network load.

Congestion control in datacenter networks. A vast literature addresses datacenter congestion through congestion control protocols [4, 22, 29, 30, 37], flow scheduling [3, 5, 25, 41, 42], and coflow abstractions [2, 11–13, 74]. MonkeyTree takes a complementary approach, managing congestion through placement and migration rather than network-layer mechanisms.

CPU migration. CPU migration is well studied for load balancing in shared clusters [16, 24, 69], though later work adopted more conservative policies as datacenter-scale deployments exposed migration overheads [61, 64]. The most closely related line of work jointly optimizes placement and routing, balancing migration cost and network congestion [28, 32, 33]. MonkeyTree decouples this tradeoff: operators specify a target network load, and MonkeyTree computes the minimum number of migrations required to meet it.

GPU migration. Prior work on GPU migration falls into two categories. The first focuses on efficient migration mechanisms: systems such as TrainMover enable live migration with minimal training disruption [21, 36]. MonkeyTree instead adopts a lightweight checkpoint-and-restore approach that buffers state in CPU memory rather than on disk; these techniques are orthogonal and would reduce migration overhead in MonkeyTree. The second targets GPU resource defragmentation and fine-grained allocation at the granularity of individual GPUs or MIG partitions [70, 71]. MonkeyTree targets large-scale training jobs that occupy entire servers, where contention manifests in the network rather than at the device level.

Elastic training. Elastic training allows workers to dynamically join and leave a training job to improve fault tolerance and utilization [17, 23, 34]. Such mechanisms complement MonkeyTree’s migrations by reducing the associated disruption.

10 CONCLUSION

We presented MonkeyTree, a migration-based defragmentation system that mitigates network congestion in multi-tenant GPU clusters. Our evaluation shows that MonkeyTree improves average job completion time by 14% over the next-best baseline and keeps p99 slowdown to 5% at 16:1 oversubscription on 2,048 GPUs, with a 9.02 s migration overhead per worker via in-memory RDMA checkpoint-and-restore.

ACKNOWLEDGMENTS

Thank you to Hari Balakrishnan, Jeremy Carin, Om Chabra, Sneha Deep Gayen, Sanjoli Narang, and Benny Rubin for comments on early versions of this paper. This research was supported by NSF FMITF-2421734, NSF CAREER-2144766, NSF PPoSS-2217099, NSF CNS-2211382, Jane Street, and Sloan fellowship FG-2022-18504.

REFERENCES

- [1] 2021. NVIDIA A100 Tensor Core GPU. (2021). <https://www.nvidia.com/en-us/data-center/a100/>.
- [2] Saksham Agarwal, Shijin Rajakrishnan, Akshay Narayan, Rachit Agarwal, David Shmoys, and Amin Vahdat. 2018. Sincronia: near-optimal network design for coflows. In *Proceedings of the 2018 Conference of the ACM Special Interest Group on Data Communication (SIGCOMM '18)*. Association for Computing Machinery, New York, NY, USA, 16–29. <https://doi.org/10.1145/3230543.3230569>
- [3] Mohammad Al-Fares, Sivasankar Radhakrishnan, Barath Raghavan, Nelson Huang, and Amin Vahdat. 2010. Hedera: dynamic flow scheduling for data center networks. In *Proceedings of the 7th USENIX Conference on Networked Systems Design and Implementation (NSDI'10)*. USENIX Association, USA, 19.
- [4] Mohammad Alizadeh, Albert Greenberg, David A. Maltz, Jitendra Padhye, Parveen Patel, Balaji Prabhakar, Sudipta Sengupta, and Murari Sridharan. 2010. Data center TCP (DCTCP). In *Proceedings of the ACM SIGCOMM 2010 Conference (SIGCOMM '10)*. Association for

Computing Machinery, New York, NY, USA, 63–74. <https://doi.org/10.1145/1851182.1851192>

[5] Mohammad Alizadeh, Shuang Yang, Milad Sharif, Sachin Katti, Nick McKeown, Balaji Prabhakar, and Scott Shenker. 2013. pFabric: minimal near-optimal datacenter transport. In *Proceedings of the ACM SIGCOMM 2013 Conference on SIGCOMM (SIGCOMM '13)*. Association for Computing Machinery, New York, NY, USA, 435–446. <https://doi.org/10.1145/2486001.2486031>

[6] Thomas Bonald, Laurent Massoulié, Alexandre Proutiere, and Jorma Virtamo. 2006. A Queueing Analysis of Max-Min Fairness, Proportional Fairness and Balanced Fairness. *Queueing Systems* 53 (06 2006), 65–84. <https://doi.org/10.1007/s11134-006-7587-7>

[7] Broadcom. [n. d.]. *Broadcom Introduces Industry's First 800G AI Ethernet NIC*. Broadcom. <https://investors.broadcom.com/node/63641/pdf>

[8] Tom B. Brown, Benjamin Mann, Nick Ryder, Melanie Subbiah, Jared Kaplan, Prafulla Dhariwal, Arvind Neelakantan, Pranav Shyam, Girish Sastry, Amanda Askell, Sandhini Agarwal, Ariel Herbert-Voss, Gretchen Krueger, Tom Henighan, Rewon Child, Aditya Ramesh, Daniel M. Ziegler, Jeffrey Wu, Clemens Winter, Christopher Hesse, Mark Chen, Eric Sigler, Mateusz Litwin, Scott Gray, Benjamin Chess, Jack Clark, Christopher Berner, Sam McCandlish, Alec Radford, Ilya Sutskever, and Dario Amodei. 2020. Language Models are Few-Shot Learners. *CoRR* abs/2005.14165 (2020). arXiv:2005.14165 <https://arxiv.org/abs/2005.14165>

[9] Jiamin Cao, Yu Guan, Kun Qian, Jiaqi Gao, Wencong Xiao, Jianbo Dong, Binzhang Fu, Dennis Cai, and Ennan Zhai. 2024. Crux: GPU-Efficient Communication Scheduling for Deep Learning Training. In *Proceedings of the ACM SIGCOMM 2024 Conference (ACM SIGCOMM '24)*. Association for Computing Machinery, New York, NY, USA, 1–15. <https://doi.org/10.1145/3651890.3672239>

[10] Annie I. Chen and Stephen C. Graves. 2014. Sparsity-Constrained Transportation Problem. (2014). arXiv:math.OC/1402.2309 <https://arxiv.org/abs/1402.2309>

[11] Mosharaf Chowdhury and Ion Stoica. 2012. Coflow: A Networking Abstraction for Cluster Applications. In *Proceedings of the 11th ACM Workshop on Hot Topics in Networks (HotNets-XI)*. Association for Computing Machinery, New York, NY, USA, 31–36. <https://doi.org/10.1145/2390231.2390237>

[12] Mosharaf Chowdhury and Ion Stoica. 2015. Efficient Coflow Scheduling Without Prior Knowledge. In *Proceedings of the 2015 ACM Conference on Special Interest Group on Data Communication (SIGCOMM '15)*. Association for Computing Machinery, New York, NY, USA, 393–406. <https://doi.org/10.1145/2785956.2787480>

[13] Mosharaf Chowdhury, Yuan Zhong, and Ion Stoica. 2014. Efficient Coflow Scheduling with Varys. In *Proceedings of the 2014 ACM Conference on SIGCOMM (SIGCOMM '14)*. Association for Computing Machinery, New York, NY, USA, 443–454. <https://doi.org/10.1145/2619239.2626315>

[14] Cisco. [n. d.]. *Cisco Data Center Networking Solutions: Addressing the Challenges of AI/ML Infrastructure*. Cisco. <https://www.cisco.com/c/en/us/td/docs/dcn/whitepapers/cisco-addressing-ai-ml-network-challenges.html>

[15] Cisco Systems. 2025. Cisco AI Networking for Data Center with NVIDIA Spectrum-X Solution Overview. [\(2025\).](https://www.cisco.com/c/en/us/products/collateral/networking/cloud-networking-switches/nexus-9000-switches/ai-networking-dc-nvidia-spectrum-x-so.html)

[16] Christopher Clark, Keir Fraser, Steven Hand, Jacob Gorm Hansen, Eric Jul, Christian Limpach, Ian Pratt, and Andrew Warfield. 2005. Live Migration of Virtual Machines. In *2nd Symposium on Networked Systems Design & Implementation (NSDI 05)*. USENIX Association, Boston, MA. <https://www.usenix.org/conference/nsdi-05/live-migration-on-virtual-machines>

[17] Jiangfei Duan, Ziang Song, Xupeng Miao, Xiaoli Xi, Dahua Lin, Harry Xu, Minjia Zhang, and Zhihao Jia. 2024. Parcae: Proactive, Liveput-Optimized DNN Training on Preemptible Instances. In *21st USENIX Symposium on Networked Systems Design and Implementation (NSDI 24)*. USENIX Association, Santa Clara, CA, 1121–1139. <https://www.usenix.org/conference/nsdi24/presentation/duan>

[18] Aaron Grattafiori et al. at Meta. 2024. The Llama 3 Herd of Models. (2024). arXiv:cs.AI/2407.21783 <https://arxiv.org/abs/2407.21783>

[19] Adithya Gangidi, Rui Miao, Shengbao Zheng, Sai Jayesh Bondu, Guilherme Goes, Hany Morsy, Rohit Puri, Mohammad Riftadi, Ashmitha Jeevaraj Shetty, Jingyi Yang, Shuqiang Zhang, Mikel Jimenez Fernandez, Shashidhar Gandham, and Hongyi Zeng. 2024. RDMA over Ethernet for Distributed Training at Meta Scale. In *Proceedings of the ACM SIGCOMM 2024 Conference (ACM SIGCOMM '24)*. Association for Computing Machinery, New York, NY, USA, 57–70. <https://doi.org/10.1145/3651890.3672233>

[20] Soudeh Ghorbani, Yimeng Zhao, Srikanth Sundaresan, Ying Zhang, Yijing Zeng, Abhigyan Sharma, Prashanth Kannan, and Cristian Lumezanu. 2025. Congestion Patterns in a Large-scale RDMA Datacenter. In *Proceedings of the 2025 ACM Internet Measurement Conference (IMC '25)*. Association for Computing Machinery, New York, NY, USA, 944–951. <https://doi.org/10.1145/3730567.3764494>

[21] Fan Guo, Yongkun Li, John C. S. Lui, and Yinlong Xu. 2019. DCUDA: Dynamic GPU Scheduling with Live Migration Support. In *Proceedings of the ACM Symposium on Cloud Computing (SoCC '19)*. Association for Computing Machinery, New York, NY, USA, 114–125. <https://doi.org/10.1145/3357223.3362714>

[22] Sangtae Ha, Injong Rhee, and Lisong Xu. 2008. CUBIC: a new TCP-friendly high-speed TCP variant. *SIGOPS Oper. Syst. Rev.* 42, 5 (jul 2008), 64–74. <https://doi.org/10.1145/1400097.1400105>

[23] Chaoyang He, Shen Li, Mahdi Soltanolkotabi, and Salman Avestimehr. 2021. PipeTransformer: Automated Elastic Pipelining for Distributed Training of Large-scale Models. In *Proceedings of the 38th International Conference on Machine Learning (Proceedings of Machine Learning Research)*, Marina Meila and Tong Zhang (Eds.), Vol. 139. PMLR, 4150–4159. <https://proceedings.mlr.press/v139/he21a.html>

[24] Michael R. Hines and Kartik Gopalan. 2009. Post-copy based live virtual machine migration using adaptive pre-paging and dynamic self-ballooning. In *Proceedings of the 2009 ACM SIGPLAN/SIGOPS International Conference on Virtual Execution Environments (VEE '09)*. Association for Computing Machinery, New York, NY, USA, 51–60. <https://doi.org/10.1145/1508293.1508301>

[25] Chi-Yao Hong, Matthew Caesar, and P. Brighten Godfrey. 2012. Finishing flows quickly with preemptive scheduling. In *Proceedings of the ACM SIGCOMM 2012 Conference on Applications, Technologies, Architectures, and Protocols for Computer Communication (SIGCOMM '12)*. Association for Computing Machinery, New York, NY, USA, 127–138. <https://doi.org/10.1145/2342356.2342389>

[26] John E. Hopcroft and Richard M. Karp. 1973. An $n^{5/2}$ Algorithm for Maximum Matchings in Bipartite Graphs. *SIAM J. Comput.* 2, 4 (1973), 225–231. <https://doi.org/10.1137/0202019> arXiv:<https://doi.org/10.1137/0202019>

[27] Christian Hopps. 2000. Analysis of an Equal-Cost Multi-Path Algorithm. RFC 2992. (Nov. 2000). <https://doi.org/10.17487/RFC2992>

[28] Hirofumi Ichihara, Yuki Koizumi, Hiroyuki Ohsaki, Kunio Hato, Junichi Murayama, and Makoto Imase. 2012. On the integrated control of virtual machine live migration and traffic engineering for cloud computing. In *2012 IEEE Global Communications Conference (GLOBECOM)*, 1629–1634. <https://doi.org/10.1109/GLOCOM.2012.6503347>

[29] V. Jacobson. 1988. Congestion avoidance and control. *SIGCOMM Comput. Commun. Rev.* 18, 4 (aug 1988), 314–329. <https://doi.org/10.1145/52325.52356>

[30] V. Jacobson. 1988. Congestion avoidance and control. In *Symposium Proceedings on Communications Architectures and Protocols (SIGCOMM '88)*. Association for Computing Machinery, New York, NY, USA, 314–329. <https://doi.org/10.1145/52324.52356>

[31] Morris A. Jette and Tim Wickberg. 2023. Architecture of the Slurm Workload Manager. In *Job Scheduling Strategies for Parallel Processing: 26th Workshop, JSSPP 2023, St. Petersburg, FL, USA, May 19, 2023, Revised Selected Papers*. Springer-Verlag, Berlin, Heidelberg, 3–23. https://doi.org/10.1007/978-3-031-43943-8_1

[32] Joe Wenjie Jiang, Tian Lan, Sangtae Ha, Minghua Chen, and Mung Chiang. 2012. Joint VM placement and routing for data center traffic engineering. In *2012 Proceedings IEEE INFOCOM*. 2876–2880. <https://doi.org/10.1109/INFCOM.2012.6195719>

[33] Renuga Kanagavelu, Bu-Sung Lee, Nguyen The Dat Le, Luke Ng Mingjie, and Khin Mi Mi Aung. 2014. Virtual machine placement with two-path traffic routing for reduced congestion in data center networks. *Computer Communications* 53 (2014), 1–12. <https://doi.org/10.1016/j.comcom.2014.07.009>

[34] Xueze Kang, Guangyu Xiang, Yuxin Wang, Hao Zhang, Yuchu Fang, Yuhang Zhou, Zhenheng Tang, Youhui Lv, Eliran Maman, Mark Wasserman, Alon Zameret, Zhipeng Bian, Shushu Chen, Zhiyou Yu, Jin Wang, Xiaoyu Wu, Yang Zheng, Chen Tian, and Xiaowen Chu. 2025. ElasWave: An Elastic-Native System for Scalable Hybrid-Parallel Training. (2025). arXiv:cs.DC/2510.00606 <https://arxiv.org/abs/2510.00606>

[35] A. H. Land and A. G. Doig. 1960. An Automatic Method of Solving Discrete Programming Problems. *Econometrica* 28, 3 (1960), 497–520. <http://www.jstor.org/stable/1910129>

[36] ChonLam Lao, Minlan Yu, Aditya Akella, Jiamin Cao, Yu Guan, Pengcheng Zhang, Zhilong Zheng, Yichi Xu, Ennan Zhai, Dennis Cai, and Jiaqi Gao. 2025. TrainMover: An Interruption-Resilient and Reliable ML Training Runtime. (2025). arXiv:cs.DC/2412.12636 <https://arxiv.org/abs/2412.12636>

[37] Yuliang Li, Rui Miao, Hongqiang Harry Liu, Yan Zhuang, Fei Feng, Lingbo Tang, Zheng Cao, Ming Zhang, Frank Kelly, Mohammad Alizadeh, and Minlan Yu. 2019. HPCC: high precision congestion control. In *Proceedings of the ACM Special Interest Group on Data Communication (SIGCOMM '19)*. Association for Computing Machinery, New York, NY, USA, 44–58. <https://doi.org/10.1145/3341302.3342085>

[38] Yadong Liu, Yunming Xiao, Xuan Zhang, Weizhen Dang, Huihui Liu, Xiang Li, Zekun He, Jilong Wang, Aleksandar Kuzmanovic, Ang Chen, and Congcong Miao. 2025. Unlocking ECMP programmability for precise traffic control. In *Proceedings of the 22nd USENIX Symposium on Networked Systems Design and Implementation (NSDI '25)*. USENIX Association, USA, Article 6, 20 pages.

[39] Meta. [n. d.]. *Llama-2-70b*. Meta. <https://huggingface.co/meta-llama/Llama-2-70b>

[40] Meta. [n. d.]. *Meta-Llama-3-70B*. Meta. <https://huggingface.co/meta-llama/Meta-Llama-3-70B>

[41] Radhika Mittal, Rachit Agarwal, Sylvia Ratnasamy, and Scott Shenker. 2016. Universal Packet Scheduling. In *13th USENIX Symposium on Networked Systems Design and Implementation (NSDI 16)*. USENIX Association, Santa Clara, CA, 501–521. <https://www.usenix.org/conference/nsdi16/technical-sessions/presentation/mittal>

[42] Behnam Montazeri, Yilong Li, Mohammad Alizadeh, and John Ousterhout. 2018. Homa: a receiver-driven low-latency transport protocol using network priorities. In *Proceedings of the 2018 Conference of the ACM Special Interest Group on Data Communication (SIGCOMM '18)*. Association for Computing Machinery, New York, NY, USA, 221–235. <https://doi.org/10.1145/3230543.3230564>

[43] Deepak Narayanan, Mohammad Shoeybi, Jared Casper, Patrick LeGresley, Mostofa Patwary, Vijay Korthikanti, Dmitri Vainbrand, Prethvi Kashinkunti, Julie Bernauer, Bryan Catanzaro, Amar Phanishayee, and Matei Zaharia. 2021. Efficient large-scale language model training on GPU clusters using megatron-LM. In *Proceedings of the International Conference for High Performance Computing, Networking, Storage and Analysis (SC '21)*. Association for Computing Machinery, New York, NY, USA, Article 58, 15 pages. <https://doi.org/10.1145/3458817.3476209>

[44] Nvidia. [n. d.]. *ConnectX-5*. Nvidia. <https://www.nvidia.com/en-sg/networking/ethernet/connectx-5/>

[45] Nvidia. [n. d.]. *NVIDIA DGX SuperPOD: Next Generation Scalable Infrastructure for AI Leadership*. Nvidia. [https://docs.nvidia.com/dgx-superpod-reference-architecture-dgx-h100.pdf](https://docs.nvidia.com/https://docs.nvidia.com/dgx-superpod-reference-architecture-dgx-h100.pdf)

[46] Nvidia. [n. d.]. *Optimize Large-Scale AI Workloads with NVIDIA Spectrum-X*. Nvidia. <https://developer.nvidia.com/blog/optimize-large-scale-ai-workloads-with-nvidia-spectrum-x/>

[47] Nvidia. [n. d.]. *Powering Next-Generation AI Networking with NVIDIA SuperNICs*. Nvidia. <https://developer.nvidia.com/blog/powering-next-generation-ai-networking-with-nvidia-superNICs>

[48] Nvidia. 2023. NVLink and NVSwitch: The building blocks of advanced multi-GPU communication—within and between servers. (2023). <https://www.nvidia.com/en-us/data-center/nvlink/>

[49] OpenAI. [n. d.]. *gpt-oss-120b*. OpenAI. <https://huggingface.co/openai/gpt-oss-120b>

[50] OpenAI. [n. d.]. *gpt-oss-20b*. OpenAI. <https://huggingface.co/openai/gpt-oss-20b>

[51] OpenAI, ;, Sandhini Agarwal, Lama Ahmad, Jason Ai, Sam Altman, Andy Applebaum, Edwin Arbus, Rahul K. Arora, Yu Bai, Bowen Baker, Haiming Bao, Boaz Barak, Ally Bennett, Tyler Bertao, Nivedita Brett, Eugene Brevdo, Greg Brockman, Sebastian Bubeck, Che Chang, Kai Chen, Mark Chen, Enoch Cheung, Aidan Clark, Dan Cook, Marat Dukhan, Casey Dvorak, Kevin Fives, Vlad Fomenko, Timur Garipov, Kristian Georgiev, Mia Glaese, Tarun Gogineni, Adam Goucher, Lukas Gross, Katia Gil Guzman, John Hallman, Jackie Hehir, Johannes Heidecke, Alec Helyar, Haitang Hu, Romain Huet, Jacob Huh, Saachi Jain, Zach Johnson, Chris Koch, Irina Kofman, Dominik Kundel, Jason Kwon, Volodymyr Kyrylov, Elaine Ya Le, Guillaume Leclerc, James Park Lennon, Scott Lessans, Mario Lezcano-Casado, Yuanzhi Li, Zhuohan Li, Ji Lin, Jordan Liss, Lily Liu, Jiancheng Liu, Kevin Lu, Chris Lu, Zoran Martinovic, Lindsay McCallum, Josh McGrath, Scott McKinney, Aidan McLaughlin, Song Mei, Steve Mostovoy, Tong Mu, Gideon Myles, Alexander Neitz, Alex Nichol, Jakub Pachocki, Alex Paino, Dana Palmie, Ashley Pantuliano, Giambattista Parascandolo, Jongsoo Park, Leher Pathak, Carolina Paz, Ludovic Peran, Dmitry Pimenov, Michelle Pokrass, Elizabeth Proehl, Huida Qiu, Gaby Raila, Filippo Raso, Hongyu Ren, Kimmy Richardson, David Robinson, Bob Rotsted, Hadi Salman, Suvansh Sanjeev, Max Schwarzer, D. Sculley, Harshit Sikchi, Kendal Simon, Karan Singhal, Yang Song, Dane Stuckey, Zhiqiang Sun, Philippe Tillet, Sam Toizer, Foivos Tsimpourlas, Nikhil Vyas, Eric Wallace, Xin Wang, Miles Wang, Olivia Watkins, Kevin Weil, Amy Wendling, Kevin Whinnery, Cedric Whitney, Hannah Wong, Lin Yang, Yu Yang, Michihiro Yasunaga, Kristen Ying, Wojciech Zaremba, Wenting Zhan, Cyril Zhang, Brian Zhang, Eddie Zhang, and Shengjia Zhao. 2025. *gpt-oss-120b & gpt-oss-20b Model Card*. (2025). arXiv:cs.CL/2508.10925 <https://arxiv.org/abs/2508.10925>

[52] PyTorch Documentation. 2025. *Distributed Checkpoint — torch.distributed.checkpoint*. PyTorch. <https://docs.pytorch.org/docs/stable/distributed/distributed.checkpoint.html> Last updated October 8, 2025.

[53] Chenchen Qi, Wenfei Wu, Yongcan Wang, Keqiang He, Yu-Hsiang (Sean) Kao, Zongying He, Chen-Yu Yen, Zhuo Jiang, Feng Luo, Surendra Anubolu, Yanjin Gao, Bingfeng Lin, Wenda Ni, Yiming Yang, Donglin Wei, Boyang Zhou, Jian Wang, and Shan Ding. 2025.

SGLB: Scalable and Robust Global Load Balancing in Commodity AI Clusters. In *Proceedings of the ACM SIGCOMM 2025 Conference (SIGCOMM '25)*. Association for Computing Machinery, New York, NY, USA, 626–644. <https://doi.org/10.1145/3718958.3750527>

[54] Kun Qian, Yongqing Xi, Jiamin Cao, Jiaqi Gao, Yichi Xu, Yu Guan, Binzhang Fu, Xuemei Shi, Fangbo Zhu, Rui Miao, Chao Wang, Peng Wang, Pengcheng Zhang, Xianlong Zeng, Eddie Ruan, Zhiping Yao, Ennan Zhai, and Dennis Cai. 2024. Alibaba HPN: A Data Center Network for Large Language Model Training. In *Proceedings of the ACM SIGCOMM 2024 Conference (ACM SIGCOMM '24)*. Association for Computing Machinery, New York, NY, USA, 691–706. <https://doi.org/10.1145/3651890.3672265>

[55] Sudarsanan Rajasekaran, Manya Ghobadi, and Aditya Akella. 2024. CASSINI: Network-Aware Job Scheduling in Machine Learning Clusters. In *21st USENIX Symposium on Networked Systems Design and Implementation (NSDI 24)*. USENIX Association, Santa Clara, CA, 1403–1420. <https://www.usenix.org/conference/nsdi24/presentation/rjasekaran>

[56] Sudarsanan Rajasekaran, Manya Ghobadi, Gautam Kumar, and Aditya Akella. 2022. Congestion control in machine learning clusters. In *Proceedings of the 21st ACM Workshop on Hot Topics in Networks (HotNets '22)*. Association for Computing Machinery, New York, NY, USA, 235–242. <https://doi.org/10.1145/3563766.3564115>

[57] Sudarsanan Rajasekaran, Sanjoli Narang, Anton A. Zabreyko, and Manya Ghobadi. 2024. MLTCP: A Distributed Technique to Approximate Centralized Flow Scheduling For Machine Learning. In *Proceedings of the 23rd ACM Workshop on Hot Topics in Networks (HotNets '24)*. Association for Computing Machinery, New York, NY, USA, 167–176. <https://doi.org/10.1145/3696348.3696878>

[58] Sudarsanan Rajasekaran, Sanjoli Narang, Anton A. Zabreyko, and Manya Ghobadi. 2024. MLTCP: Congestion Control for DNN Training. (2024). arXiv:cs.NI/2402.09589 <https://arxiv.org/abs/2402.09589>

[59] Hossein Shafeirad, Amir Shani, Manaf Bin-Yahya, Seyed Hossein Mortazavi, Geng Li, Xinh Du, Tao Su, Wei Wang, Jingbin Zhou, and Majid Ghaderi. 2025. Harmonics: Scalable Collective Scheduling in Multi-Tenant GPU Clusters. *Proc. ACM Netw.* 3, CoNEXT4, Article 38 (Nov. 2025), 20 pages. <https://doi.org/10.1145/3768985>

[60] Min Si, Pavan Balaji, Yongzhou Chen, Ching-Hsiang Chu, Adi Gangidi, Saif Hasan, Subodh Iyengar, Dan Johnson, Bingzhe Liu, Regina Ren, Deep Shah, Ashmitha Jeevaraj Shetty, Greg Steinbrecher, Yulun Wang, Bruce Wu, Xinfeng Xie, Jingyi Yang, Mingran Yang, Kenny Yu, Minlan Yu, Cen Zhao, Wes Bland, Denis Boyda, Suman Gumudavelli, Prashanth Kannan, Cristian Lumezanu, Rui Miao, Zhe Qu, Venkat Ramesh, Maxim Samoylov, Jan Seidel, Srikanth Sundaresan, Feng Tian, Qiye Tan, Shuqiang Zhang, Yimeng Zhao, Shengbao Zheng, Art Zhu, and Hongyi Zeng. 2026. Collective Communication for 100k+ GPUs. (2026). arXiv:cs.DC/2510.20171 <https://arxiv.org/abs/2510.20171>

[61] Orathai Sukwong and Hyong S. Kim. 2011. Is co-scheduling too expensive for SMP VMs?. In *Proceedings of the Sixth Conference on Computer Systems (EuroSys '11)*. Association for Computing Machinery, New York, NY, USA, 257–272. <https://doi.org/10.1145/1966445.1966469>

[62] Hugo Touvron, Louis Martin, Kevin Stone, Peter Albert, Amjad Almahairei, Yasmine Babaei, Nikolay Bashlykov, Soumya Batra, Prajjwal Bhargava, Shruti Bhosale, Dan Biket, Lukas Blecher, Cristian Canton Ferrer, Moya Chen, Guillem Cucurull, David Esiobu, Jude Fernandes, Jeremy Fu, Wenjin Fu, Brian Fuller, Cynthia Gao, Vedanuj Goswami, Naman Goyal, Anthony Hartshorn, Saghar Hosseini, Rui Hou, Hakan Inan, Marcin Kardas, Viktor Kerkez, Madian Khabsa, Isabel Kloumann, Artem Korenev, Punit Singh Koura, Marie-Anne Lachaux, Thibault Lavril, Jenya Lee, Diana Liskovich, Yinghai Lu, Yuning Mao, Xavier Martinet, Todor Mihaylov, Pushkar Mishra, Igor Molybog, Yixin Nie, Andrew Poulton, Jeremy Reizenstein, Rashi Rungta, Kalyan Saladi, Alan Schelten, Ruan Silva, Eric Michael Smith, Ranjan Subramanian, Xiaoqing Ellen Tan, Binh Tang, Ross Taylor, Adina Williams, Jian Xiang Kuan, Puxin Xu, Zheng Yan, Iliyan Zarov, Yuchen Zhang, Angela Fan, Melanie Kambadur, Sharan Narang, Aurelien Rodriguez, Robert Stojnic, Sergey Edunov, and Thomas Scialom. 2023. Llama 2: Open Foundation and Fine-Tuned Chat Models. (2023). arXiv:cs.CL/2307.09288 <https://arxiv.org/abs/2307.09288>

[63] Ultra Ethernet Consortium. [n. d.]. *UEC 1.0: NEW HIGH-PERFORMANCE STANDARD FOR SCALING HPC-AI*. Ultra Ethernet Consortium. <https://ultraethernet.org/wp-content/uploads/sites/20/2025/06/UEC1.0Whitepaper.pdf>

[64] Manohar Vanga, Arpan Gujarati, and Björn B. Brandenburg. 2018. Tableau: a high-throughput and predictable VM scheduler for high-density workloads. In *Proceedings of the Thirteenth EuroSys Conference (EuroSys '18)*. Association for Computing Machinery, New York, NY, USA, Article 28, 16 pages. <https://doi.org/10.1145/3190508.3190557>

[65] Weiyang Wang, Manya Ghobadi, Kayvon Shakeri, Ying Zhang, and Naader Hasani. 2024. Rail-only: A Low-Cost High-Performance Network for Training LLMs with Trillion Parameters. In *2024 IEEE Symposium on High-Performance Interconnects (HOTI)*. 1–10. <https://doi.org/10.1109/HOTI63208.2024.00013>

[66] Xizheng Wang, Qingxu Li, Yichi Xu, Gang Lu, Dan Li, Li Chen, Heyang Zhou, Linkang Zheng, Sen Zhang, Yikai Zhu, Yang Liu, Pengcheng Zhang, Kun Qian, Kunling He, Jiaqi Gao, Ennan Zhai, Dennis Cai, and Binzhang Fu. 2025. SimAI: Unifying Architecture Design and Performance Tuning for Large-Scale Large Language Model Training with Scalability and Precision. In *22nd USENIX Symposium on Networked Systems Design and Implementation (NSDI 25)*. USENIX Association, Philadelphia, PA, 541–558. <https://www.usenix.org/conference/nsdi25/presentation/wang-xizheng-simai>

[67] Qizhen Weng, Wencong Xiao, Yinghao Yu, Wei Wang, Cheng Wang, Jian He, Yong Li, Liping Zhang, Wei Lin, and Yu Ding. 2022. MLaaS in the Wild: Workload Analysis and Scheduling in Large-Scale Heterogeneous GPU Clusters. In *19th USENIX Symposium on Networked Systems Design and Implementation (NSDI 22)*. USENIX Association, Renton, WA, 945–960. <https://www.usenix.org/conference/nsdi22/presentation/weng>

[68] William Won, Taekyung Heo, Saeed Rashidi, Srinivas Sridharan, Sudarshan Srinivasan, and Tushar Krishna. 2023. ASTRA-sim2.0: Modeling Hierarchical Networks and Disaggregated Systems for Large-model Training at Scale. In *2023 IEEE International Symposium on Performance Analysis of Systems and Software (ISPASS)*. 283–294. <https://doi.org/10.1109/ISPASS57527.2023.00035>

[69] Timothy Wood, Prashant Shenoy, and Mazin Yousif. 2007. Black-box and Gray-box Strategies for Virtual Machine Migration. In *4th USENIX Symposium on Networked Systems Design & Implementation (NSDI 07)*. USENIX Association, Cambridge, MA. <https://www.usenix.org/conference/nsdi-07/black-box-and-gray-box-strategies-virtual-machine-migration>

[70] Qingfu Wu, Pengfei Chen, and Yilun Wang. 2026. Defragmentation Scheduling with Deep Reinforcement Learning in Shared GPU Clusters. In *Proceedings of the 2025 ACM Symposium on Cloud Computing (SoCC '25)*. Association for Computing Machinery, New York, NY, USA, 402–415. <https://doi.org/10.1145/3772052.3772242>

[71] Wencong Xiao, Romil Bhardwaj, Ramachandran Ramjee, Muthian Sivathanu, Nipun Kwatra, Zhenhua Han, Pratyush Patel, Xuan Peng, Hanyu Zhao, Quanlu Zhang, Fan Yang, and Lidong Zhou. 2018. Gandiva: Introspective Cluster Scheduling for Deep Learning. In *13th USENIX Symposium on Operating Systems Design and Implementation (OSDI 18)*. USENIX Association, Carlsbad, CA, 595–610. <https://www.usenix.org/conference/osdi18/presentation/xiao>

- [72] Wencong Xiao, Shiru Ren, Yong Li, Yang Zhang, Pengyang Hou, Zhi Li, Yihui Feng, Wei Lin, and Yangqing Jia. 2020. AntMan: Dynamic Scaling on GPU Clusters for Deep Learning. In *14th USENIX Symposium on Operating Systems Design and Implementation (OSDI 20)*. USENIX Association, 533–548. <https://www.usenix.org/conference/osdi20/presentation/xiao>
- [73] Farid Zandi Shafagh, Manya Ghobadi, and Yashar Ganjali. [n. d.]. FORESIGHT: Joint Time and Space Scheduling for Efficient Distributed ML Training. In *2025 IFIP Networking Conference (IFIP Networking 2025), Limassol, Cyprus, May 26-29, 2025*.
- [74] Hong Zhang, Li Chen, Bairen Yi, Kai Chen, Mosharaf Chowdhury, and Yanhui Geng. 2016. CODA: Toward Automatically Identifying and Scheduling Coflows in the Dark. In *Proceedings of the 2016 ACM SIGCOMM Conference (SIGCOMM '16)*. Association for Computing Machinery, New York, NY, USA, 160–173. <https://doi.org/10.1145/2934872.2934880>